



# Evaluating Production of Cyclopentyl Tetraethers by Marine Group II *Euryarchaeota* in the Pearl River Estuary and Coastal South China Sea: Potential Impact on the TEX<sub>86</sub> Paleothermometer

Jin-Xiang Wang<sup>1,2†</sup>, Wei Xie<sup>3†</sup>, Yi Ge Zhang<sup>4</sup>, Travis B. Meador<sup>1</sup> and Chuanlun L. Zhang<sup>3,5\*</sup>

<sup>1</sup> MARUM-Center for Marine Environmental Sciences, University of Bremen, Bremen, Germany, <sup>2</sup> Department of Marine Sciences, University of Georgia, Athens, GA, United States, <sup>3</sup> State Key Laboratory of Marine Geology, Tongji University, Shanghai, China, <sup>4</sup> Department of Oceanography, Texas A&M University, College Station, TX, United States, <sup>5</sup> Department of Ocean Science & Engineering, Southern University of Science and Technology, Shenzhen, China

## OPEN ACCESS

### Edited by:

Stefan M. Sievert,  
Woods Hole Oceanographic  
Institution, United States

### Reviewed by:

Florence Schubotz,  
University of Bremen, Germany  
Anitra E. Ingalls,  
University of Washington,  
United States

### \*Correspondence:

Chuanlun L. Zhang  
zhangcl@sustc.edu.cn

†These authors have contributed  
equally to this work.

### Specialty section:

This article was submitted to  
Aquatic Microbiology,  
a section of the journal  
Frontiers in Microbiology

Received: 31 May 2017

Accepted: 10 October 2017

Published: 31 October 2017

### Citation:

Wang J-X, Xie W, Zhang YG,  
Meador TB and Zhang CL (2017)  
Evaluating Production of Cyclopentyl  
Tetraethers by Marine Group II  
*Euryarchaeota* in the Pearl River  
Estuary and Coastal South China Sea:  
Potential Impact on the TEX<sub>86</sub>  
Paleothermometer.  
Front. Microbiol. 8:2077.  
doi: 10.3389/fmicb.2017.02077

TEX<sub>86</sub> [TetraEther indeX of glycerol dialkyl glycerol tetraethers (GDGTs) with 86 carbon atoms] has been widely applied to reconstruct (paleo-) sea surface temperature. Marine Group I (MG-I) *Thaumarchaeota* were thought to be the primary source of GDGTs constituting the TEX<sub>86</sub> formula; however, recent research has suggested that Marine Group II (MG-II) *Euryarchaeota* may also contribute significantly to the GDGT pool in the ocean. Little is known regarding the potential impact of MG-II *Euryarchaeota*-derived GDGTs on TEX<sub>86</sub> values recorded in marine sediments. In this study, we assessed the relationship between distributions of GDGTs and MG-II *Euryarchaeota* and evaluated its potential effect on the TEX<sub>86</sub> proxy. Lipid and DNA analyses were performed on suspended particulate matter and surface sediments collected along a salinity gradient from the lower Pearl River (river water) and its estuary (mixing water) to the coastal South China Sea (SCS, seawater). TEX<sub>86</sub>-derived temperatures from the water column and surface sediments were significantly correlated and both were lower than satellite-based temperatures. The ring index (RI) values in these environments were higher than predicted from the calculated TEX<sub>86</sub>-RI correlation, indicating that the GDGT pool in the water column of the PR estuary and coastal SCS comprises relatively more cyclopentane rings, which thereby altered TEX<sub>86</sub> values. Furthermore, the abundance of MG-II *Euryarchaeota* 16S rRNA gene in the mixing water was two to three orders of magnitude higher than those observed in the river or seawater. Significant linear correlations were observed between the gene abundance ratio of MG-II *Euryarchaeota* to total archaea and the fractional abundance of GDGTs with cyclopentane rings. Collectively, these results suggest that MG-II *Euryarchaeota* likely produce a large proportion of GDGTs with 1–4 cyclopentane moieties, which may bias TEX<sub>86</sub> values in the water column and sediments. As such, valid interpretation of TEX<sub>86</sub> values in the sediment record, particularly in coastal oceans, should consider the contribution from MG-II *Euryarchaeota*.

**Keywords:** Marine Group II, *Euryarchaeota*, GDGTs, TEX<sub>86</sub>, ring index, South China Sea

## INTRODUCTION

TEX<sub>86</sub> is a popular temperature proxy applied in paleoclimatological studies, which is based on the relative distribution of cyclopentane rings among isoprenoid glycerol dialkyl glycerol tetraether (GDGT; **Figure S1**) lipids produced by archaea in marine and terrestrial environments (see review by Schouten et al., 2013). Global core-top calibrations of TEX<sub>86</sub> values were empirically correlated with the annual mean sea surface temperature (SST; Schouten et al., 2002; Kim et al., 2008, 2010). However, mounting evidence indicates anomalies of TEX<sub>86</sub>-derived SST in coastal seas and the open ocean, which have been attributed to multiple inputs of GDGTs from terrestrial (e.g., Weijers et al., 2006) or bathypelagic sources (e.g., Lee et al., 2008), as well as production in marine sediments (e.g., Liu X. L. et al., 2011).

A great deal of effort has been made to assess TEX<sub>86</sub> accuracy in marine and lake sediments. For example, application of the TEX<sub>86</sub> proxy is cautioned under the following circumstances: a branched and isoprenoid tetraether (BIT) index > 0.2 (Zhu et al., 2011), a ratio of GDGT-2/crenarchaeol > 0.4 (Weijers et al., 2011a), a Methane Index > 0.5 (Zhang et al., 2011), a ratio of GDGT-0/crenarchaeol > 2 (Blaga et al., 2009), or when %GDGT-2 > 45 (Sinninghe Damsté et al., 2012). Recently, based on an assessment of the relationship between the weighted average number of cyclopentane rings in GDGTs (ring index, RI) and published TEX<sub>86</sub> data from core-top sediments, Zhang et al. (2016) established a significant correlation between TEX<sub>86</sub> and RI [ $RI = 3.32 \times (TEX_{86})^2 - 0.77 \times TEX_{86} + 1.59; \pm 2\sigma \sim 0.3$ ]. This relationship was expected and reflects the physiological response of marine archaea to synthesize GDGTs with more rings (higher RI values) at higher temperatures (higher TEX<sub>86</sub> values). Deviations from this relationship suggest that temperature is not a dominant factor governing GDGT ring distribution, or, alternatively, the relationship between GDGT ring distribution and temperature is different from the modern analog as defined by the global core-top dataset.

The TEX<sub>86</sub>-related GDGTs (GDGTs-1, -2, -3 and the crenarchaeol regioisomer) in the water column are thought to primarily derive from the Marine Group I (MG-I) *Thaumarchaeota* (e.g., Schouten et al., 2008; Pitcher et al., 2011a,b), as it is one of the dominant groups of planktonic archaea in the ocean (Karner et al., 2001). In particular, crenarchaeol, containing one cyclohexane and four cyclopentane moieties, is accepted as a specific biomarker for MG-I *Thaumarchaeota* (Sinninghe Damsté et al., 2002; Schouten et al., 2008). Marine Group II (MG-II) *Euryarchaeota* are another group of planktonic archaea that predominantly inhabit coastal water and (near) surface waters of the open ocean (e.g., DeLong, 1992; Galand et al., 2010; Hugoni et al., 2013). Recently, this cosmopolitan group was also invoked as another major source of GDGTs (including crenarchaeol) in the ocean (Lincoln et al., 2014a), which supports an earlier hypothesis about GDGT-producing MG-II *Euryarchaeota* (Turich et al., 2007). However, concrete evidence of crenarchaeol production by MG-II is lacking due to the inability to obtain a pure culture or isolate, and the exact composition of GDGTs produced by these

organisms remains uncertain (Lincoln et al., 2014b; Schouten et al., 2014).

To further evaluate the relationship between MG-II *Euryarchaeota* and the distribution of GDGTs, we quantified the abundance of MG-II 16S rRNA gene, determined the distribution of GDGT core and intact polar lipids (CL and IPL, respectively), and assessed TEX<sub>86</sub> and Ring Index (RI) values from suspended particulate matter and surface sediments collected from the lower Pearl River (PR) and its estuary to the coastal South China Sea (SCS). Our results provide a mechanistic explanation for deviations of the TEX<sub>86</sub> paleothermometer and have important implications for the sources of GDGTs in marine environments and probing past changes in global climate.

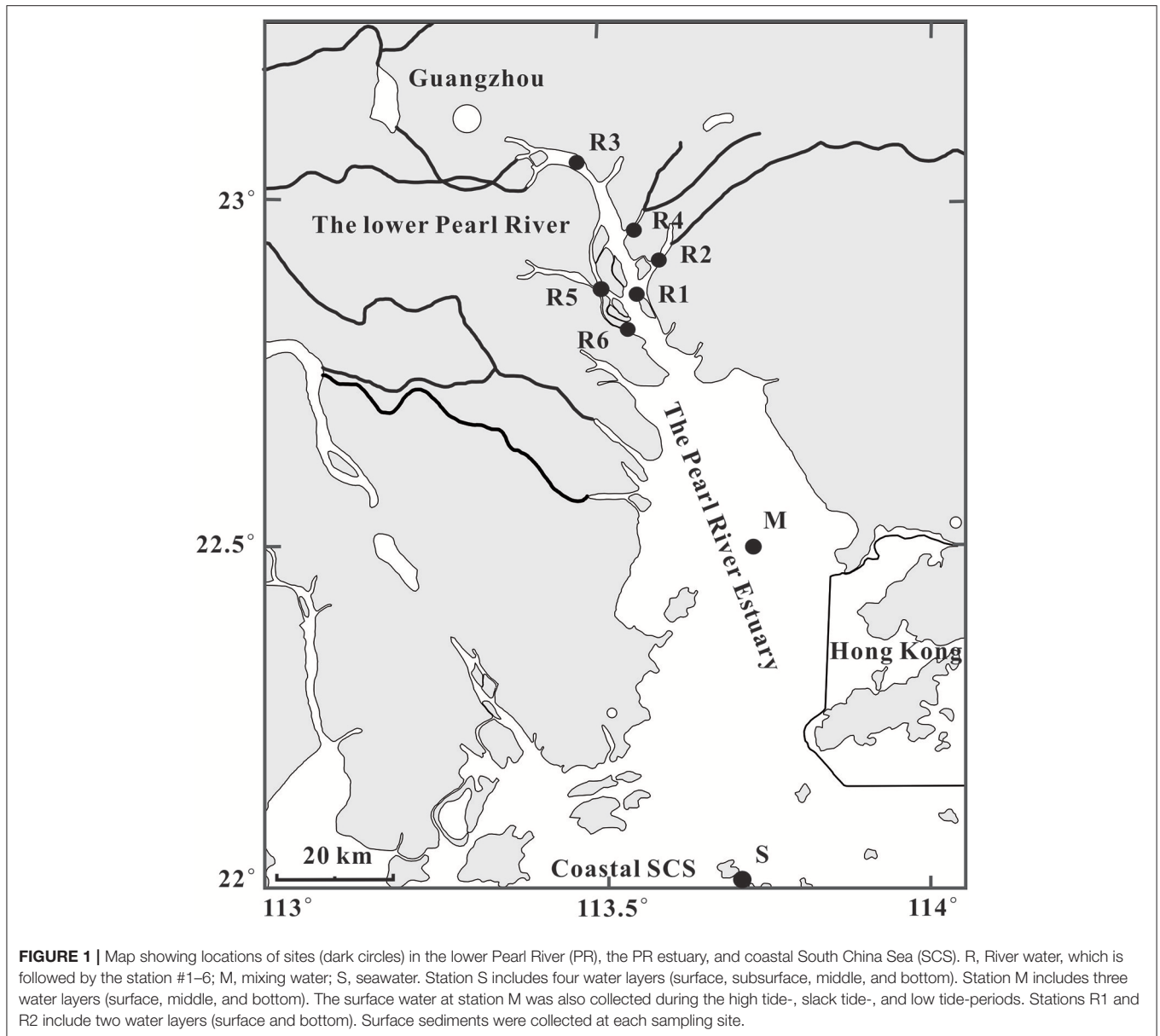
## MATERIALS AND METHODS

### Sample Collection

Sampling locations and other information for suspended particulate matter (SPM) and surface sediments are shown in **Figure 1** and **Table 1**. SPM samples ( $n = 18$ ) and surface sediments ( $n = 8$ ) were collected along a salinity gradient from the lower Pearl River and its estuary to the coastal South China Sea in the summer of 2011. SPM samples were collected from the surface (stations R1–R6) and the bottom (stations R1 and R2) water in the lower Pearl River, from three water depths (surface, middle, and bottom) and during three tidal periods (high tide, slack tide, and low tide) at station M located in the PR estuary, and at four water depths (surface, subsurface, middle, and bottom) at station S in the seawater of the coastal SCS (**Figure 1**). The depth of the sampling layers in the water column is given in **Table 1**. About 4–103 liters of water were filtered onto combusted (450°C, overnight) glass-fiber filters (Whatman GF/F, 0.7 μm, 142 mm diameter) using an *in situ* submersible pump. The pH, temperature, salinity, and depth were determined *in situ* by a Horiba instrument (W-20XD, Kyoto, Japan; **Table 1**). Surface sediments (top ca. 10 cm) were collected at all stations (**Figure 1**; **Table 1**) using a grab sampler. All samples were frozen immediately in liquid nitrogen and kept at –80°C in the laboratory before analysis.

### GDGT Extraction and Separation

The SPM samples ( $n = 18$ ) and surface sediments ( $n = 8$ ) were freeze-dried and extracted using a modified Bligh and Dyer method (Bligh and Dyer, 1959); the separation of core lipids and intact polar lipids followed the procedure described in Weijers et al. (2011b). Briefly, the total lipid extract (TLE) was obtained by ultrasonic extraction (10 min each, 6 times) of SPM (1 filter) or sediments (5 g) with a single-phase solvent mixture of methanol, dichloromethane (DCM), and phosphate buffer (2:1:0.8, v/v/v; pH 7.4). The TLE was separated over an activated silica gel column eluted with n-hexane/ethyl acetate (1:1, v/v) and methanol for CL and IPL, respectively. For GDGT quantification, a known amount of an internal C46 GDGT standard was added into the CL fraction or IPL fraction (Huguet et al., 2006). The CL fraction was directly measured. The IPL fraction was determined by measuring the CL after cleavage of the polar head groups via acid or base hydrolysis (Pitcher



et al., 2009; Weijers et al., 2011b). Briefly, 1/3 IPL fraction (non-hydrolyzed IPL fraction) was directly condensed; another 1/3 IPL fraction was hydrolyzed (2 h) in 1.5 N HCl in methanol, which was called the acid-hydrolyzed IPL fraction (total IPL). DCM and MilliQ water were added, and the DCM fraction was collected (repeated 4 times). The DCM fraction was rinsed (6 times) with MilliQ water in order to remove acid and dried under N<sub>2</sub> gas. The last 1/3 IPL fraction was subjected to base hydrolysis (2 h) in a 1 N KOH in methanol/H<sub>2</sub>O mixture (95:5, v/v), which was called the base-hydrolyzed IPL fraction (phospho IPL). Together with the condensed CL fraction, the CL fraction, two fractions of IPL-derived core lipids and non-cleaved IPL fraction were dissolved in n-hexane/isopropanol (99:1, v/v), and filtered using PTFE filters (pore diameter of 0.45 μm). The acid-hydrolyzed IPL reflected total IPL, which, prior to hydrolysis,

were attached to both phosphatidyl and glycosidic head groups; The base-hydrolyzed IPL represented IPLs with phosphatidyl head groups only (phospho IPL; Weijers et al., 2011b). Analysis of the non-hydrolyzed IPL fraction was performed to determine any carryover of CL into the IPL fraction.

### GDGT Analysis

GDGTs from all treatments were analyzed using high performance liquid chromatography-atmospheric pressure chemical ionization-tandem mass spectrometry (HPLC-APCI-MS/MS), which was performed as described by Zhang et al. (2012), using an Agilent 1200 LC equipped with an automatic injector and coupled to a QQQ 6460 MS; peaks were evaluated using Mass Hunter LC-MS manager software. Separation was achieved using a Prevail Cyano column (2.1 × 150 mm, 3 μm;

**TABLE 1** | Basic information, abundance of isoprenoid GDGTs, TEX<sub>86</sub>, Ring Index, and 16S rRNA gene abundances for suspended particulate matter (SPM) in the water column and surface sediments collected from the lower Pearl River, the Pearl River estuary, and coastal northern South China Sea.

Sample ID <sup>a</sup>	Longitude (E)	Latitude (N)	Sampling date (mm/dd/yyyy)	Depth <sup>b</sup> (m)	Temp. (°C)	Sal.	pH	isoGDGTs (ng/l) <sup>c</sup>		TEX <sub>86</sub>		Ring Index (RI) <sub>2</sub> <sup>d</sup>		Archaeal 16S (copies/l)	MG-II 16S (copies/l)	
								CL	Total-IPL	CL	Total-IPL	CL	Total-IPL			CL
<b>RIVER WATER SPM</b>																
R1_sur	113°34.249'	22°52.647'	06/21/2011	1.5	29.7	0.2	7.25	188.6	201.5	16.7	0.59	0.50	0.19	0.15	0.12	3.0E+05
R1_bot	113°34.249'	22°52.647'	06/21/2011	6.0	29.6	0.2	7.25	221.3	128.1	8.9	0.60	0.56	0.16	0.12	0.15	1.2E+03
R2_sur	113°36.680'	22°56.338'	06/21/2011	1.5	29.0	0.1	6.95	64.8	82.5	6.8	0.56	0.42	0.16	0.15	0.11	- <sup>e</sup>
R2_bot	113°36.680'	22°56.338'	06/21/2011	6.0	29.0	0.1	6.90	266.6	426.5	27.9	0.60	0.45	0.14	0.10	0.12	-
R3	113°28.726'	23°04.339'	06/22/2011	1.5	29.4	0.1	7.46	79.8	150.2	8.0	0.57	0.41	0.07	0.09	0.14	-
R4	113°33.507'	22°58.409'	06/22/2011	1.5	29.6	0.2	7.28	19.1	30.6	3.3	0.63	0.57	0.26	0.13	0.20	-
R5	113°29.941'	22°53.588'	06/22/2011	1.5	28.5	0.1	7.28	20.0	30.4	2.0	0.61	0.48	0.37	0.40	0.34	-
R6	113°33.088'	22°44.811'	06/22/2011	1.5	27.8	0.1	6.92	49.1	21.8	1.2	0.62	0.68	0.53	0.15	0.25	-
<b>MIXING WATER SPM</b>																
M_lt	113°45.098'	22°27.206'	06/18/2011	1.5	-	-	-	25.9	105.0	2.4	0.66	0.55	0.52	0.47	0.43	6.1E+06
M_st	113°45.098'	22°27.206'	06/18/2011	1.5	-	-	-	35.3	97.3	1.4	0.58	0.65	0.36	0.61	0.61	3.1E+08
M_ht	113°45.098'	22°27.206'	06/18/2011	1.5	-	-	-	21.9	86.8	2.8	0.59	0.56	0.43	0.46	0.38	1.2E+07
M_sur	113°45.098'	22°27.206'	06/18/2011	1.5	28.7	11.1	8.03	18.9	67.0	1.9	0.58	0.60	0.36	0.44	0.65	5.7E+08
M_mid	113°45.098'	22°27.206'	06/18/2011	5.0	28.3	15.6	7.93	102.6	73.4	5.2	0.61	0.64	0.35	0.47	0.36	7.9E+08
M_bot	113°45.098'	22°27.206'	06/18/2011	9.0	27.6	23.0	7.89	107.4	76.7	6.0	0.56	0.60	0.30	0.42	0.38	1.6E+09
<b>SEA WATER SPM</b>																
S_sur	113°70.448'	22°05.165'	06/15/2011	1.5	29.6	29.5	8.63	1.1	0.7	0.1	0.52	0.65	0.28	0.39	0.22	4.8E+03
S_subs	113°70.448'	22°05.165'	06/15/2011	5.0	29.5	29.7	8.64	2.1	1.1	0.1	0.56	0.63	0.27	0.33	0.24	5.3E+05
S_mid	113°70.448'	22°05.165'	06/15/2011	10.0	28.6	31.7	8.45	12.6	13.5	0.6	0.49	0.55	0.20	0.24	0.23	4.4E+03
S_bot	113°70.448'	22°05.165'	06/15/2011	18.0	25.4	33.7	7.92	21.4	9.6	0.7	0.53	0.59	0.20	0.39	0.21	1.9E+07
<b>SEDIMENT</b>																
Sedi-R1	113°34.249'	22°52.647'	06/21/2011	8.0	-	-	7.46	461.8	142.8	9.5	0.58	0.37	0.27	0.38	0.41	-
Sedi-R2	113°36.680'	22°56.338'	06/21/2011	7.0	-	-	7.68	687.5	289.2	17.0	0.56	0.35	0.23	0.22	0.26	-
Sedi-R3	113°28.726'	23°04.339'	06/22/2011	9.0	-	-	7.29	800.3	233.5	19.6	0.57	0.43	0.15	0.23	0.30	-
Sedi-R4	113°33.507'	22°58.409'	06/22/2011	7.0	-	-	7.50	881.0	149.7	9.7	0.58	0.51	0.33	0.75	0.62	-
Sedi-R5	113°29.941'	22°53.588'	06/22/2011	8.0	-	-	7.58	621.7	84.2	7.3	0.62	0.52	0.33	0.66	0.43	-
Sedi-R6	113°33.088'	22°44.811'	06/22/2011	8.0	-	-	7.66	120.2	103.8	6.2	0.67	0.35	0.42	0.65	0.74	-
Sedi-M	113°45.098'	22°27.206'	06/18/2011	12.0	-	-	7.60	200.4	67.7	2.3	0.62	0.52	0.38	0.69	0.42	-
Sedi-S	113°70.448'	21°95.165'	06/15/2011	20.0	-	-	7.40	5003.6	267.3	20.8	0.50	0.64	0.19	0.73	0.34	-

Basic information includes location, sampling date, water depth, temperature (Temp.), salinity (Sal.), and pH.

<sup>a</sup>R<sub>1</sub> River (the lower Pearl River), which is followed by the station numbers; sur and bott represent surface water and bottom water, respectively. M, Mixing water (the Pearl River estuary); lt, low tide; st, slack tide; ht, high tide; mid means middle layer water. S, Sea water (northern South China Sea); subs represents subsurface water.

<sup>b</sup>For the SPM samples collected from the water column, the depth is referred to the sampling water depth; For the sediments, the depth indicates the river water depth.

<sup>c</sup>CL, core lipids; total-IPL, intact polar lipid (IPL) derived core lipids upon acid (H) hydrolysis; phospho-IPL, IPL-derived core lipids derived upon base (OH) hydrolysis.

<sup>d</sup>RI<sub>2</sub> = [(GDGT-1) + 2\*(GDGT-2) + 3\*(GDGT-3) + 4\*(GDGT-4) + 4\*(Cren.iso)]/100.

<sup>e</sup>-, data are not available or not examined.

Alltech Deerfield, IL, USA) with n-hexane (solvent A) and a mixture of n-hexane/isopropanol 90/10 (v/v; solvent B). The (M+H)<sup>+</sup> ions of each core isoprenoid GDGT (m/z 1,302, 1,300, 1,298, 1,296, 1,294, 1,292) were monitored via selected ion monitoring (SIM) mode (Schouten et al., 2007).

## GDGT-Based Indices

Indices based on the fractional abundance of GDGTs were calculated as follows:

$$\text{TEX}_{86} = \frac{([\text{GDGT} - 2] + [\text{GDGT} - 3] + [\text{Cren.iso}])}{([\text{GDGT} - 1] + [\text{GDGT} - 2] + [\text{GDGT} - 3] + [\text{Cren.iso}])} \quad (\text{Schouten et al., 2002}) \quad (1)$$

$$\text{Ring Index}_1 (\text{RI}_1) = \frac{([\text{GDGT} - 1] + 2 \times [\text{GDGT} - 2] + 3 \times [\text{GDGT} - 3] + 4 \times [\text{Cren.}] + 4 \times [\text{Cren.iso}])}{100} \quad (\text{Zhang et al., 2016}) \quad (2)$$

$$\text{Ring Index} (\text{RI}_2) = \frac{([\text{GDGT} - 1] + 2 \times [\text{GDGT} - 2] + 3 \times [\text{GDGT} - 3] + 4 \times [\text{GDGT} - 4] + 4 \times [\text{Cren.iso}])}{100} \quad (3)$$

with the GDGT numbers corresponding to the GDGT structures in **Figure S1**. Note that  $\text{RI}_2$  was originally developed for the current study and modified from  $\text{RI}_1$  (Zhang et al., 2016), in which the fractional abundance of crenarchaeol was replaced by GDGT-4 in order to eliminate the influence of crenarchaeol on weighted average number of cyclopentane rings in GDGTs.

## DNA Extraction and the Quantitative Polymerase Chain Reaction (qPCR)

The SPM samples ( $n = 12$ ) from station R1 (river water), station M (mixing water), and station S (seawater) were selected for the DNA analysis. The frozen filters were washed 3 times by phosphate buffered saline (pH 7.4). The supernatants were centrifuged under 11,000 g for 10 min. The DNA was extracted following the protocol of FastDNA SPIN Kit. The DNA samples were dissolved with a final dilution in 100- $\mu$ L deionized water and preserved at  $-80^\circ\text{C}$  until further processing. The DNA concentrations were quantified in duplicate with a Nano-Drop spectrophotometer (Thermo Fisher Scientific Inc., Wilmington, DE, USA). The quantitative PCR primers were Arch\_334F (5'ACGGGGCGCAGCAGGCGCGA3')/Arch\_518R (5'ATTACCGCGGCTGCTGG3') for total archaeal 16S gene quantification (Bano et al., 2004), GII-554-f (5'GTCGTTTTTATTGGGCTAA3'), and Eury806-r (5'CACAGCGTTTACACCTAG3') for MG-II *Euryarchaeota* 16S gene quantification (Massana et al., 1997; Teira et al., 2004). The qPCR analysis was performed at  $95^\circ\text{C}$  for 30 s and 40 cycles at  $94^\circ\text{C}$  for 30 s,  $55^\circ\text{C}$  for total archaea and  $53^\circ\text{C}$  for MG-II *Euryarchaeota* for 30 s and  $68^\circ\text{C}$  for 1 min. Triplicate measurements were run for each sample and standard.

PCR bands of 16S rRNA gene and MG-II gene were amplified from SPM samples in Station M. They were recovered by a Gel Extraction Kit (omega) and sequenced on the 3730-sequencing platform. The sequences were annotated as the corresponding target genes, which demonstrated the specificity of

the chosen qPCR primers. A dilution series of purified DNA from those positive clones were used as standards. A melting curve analysis was performed to demonstrate that the fluorescent signal obtained in a given reaction was consistent with the expected profile for specific PCR products. The  $R^2$  values of standard curves were  $>0.99$ . The efficiency of each qPCR was between 87 and 99%.

## Amplicon Sequencing of the Archaeal 16S rRNA Gene

SPM samples collected in river water, mixing water and seawater were selected to conduct MiSeq pyrosequencing targeting the archaeal 16S rRNA gene. In contrast to the qPCR primers, these primers targeted longer sequences to increase the precision of phylogenetic analysis. The primers were Arch\_344F (5'ACGGGGCGCAGCAGGCGCGA3') and Arch\_915R (5'GTGCTCCCCCGCCAATTCCT3'; Gantner et al., 2011). The MiSeq sequencing was conducted on the MiSeq platform ( $2 \times 250$  PE, Illumina) at the Shanghai Personalbio Biotechnology (Shanghai, China). Mothur (version 1.29.2; Schloss et al., 2009) was applied to filter the raw pyrosequencing data. The selected sequences were analyzed using the QIIME standard pipeline (Caporaso et al., 2010). Taxonomy was assigned according to the Ribosomal Database Project (RDP) classifier 2.2 (minimum confidence of 80%; Cole et al., 2009). The GenBank accession numbers are PRJNA38421 for those archaeal 16S rRNA genes.

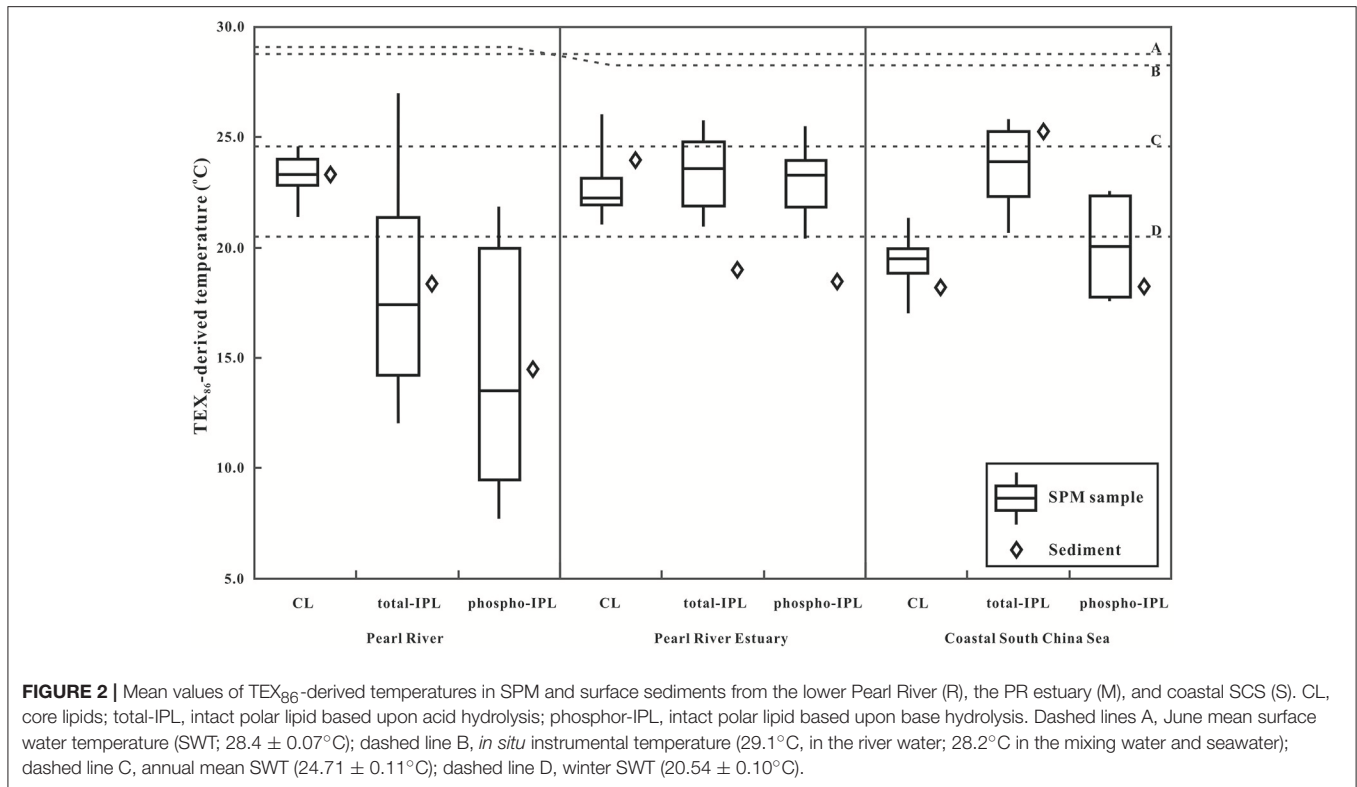
## Satellite-Derived Surface Water Temperature (SWT)

The satellite-derived SWT was determined with a spatial resolution of 4 km from the NOAA advanced very-high-resolution radiometer (AVHRR; version 5.2; <http://www.nodc.noaa.gov/SatelliteData/pathfinder4km/>). The June mean SWT was obtained from the daily averaged values of 30 days in June 2011 (sampling month). The annual mean SWT and winter mean SWT represented 8-year mean values of annual mean temperature (2004–2011) and monthly mean temperature (December–February), respectively, as the surface sediment (top ca. 10 cm) collected in this study might represent a deposition of 6–10 years, based on an estimation from Strong et al. (2012).

## RESULTS AND DISCUSSION

### TEX<sub>86</sub>-Derived Temperature and Ring Index

The  $\text{TEX}_{86}$ -derived temperature was calculated based on the calibration of Kim et al. [ $\text{SST} = 68.4 \times \log(\text{TEX}_{86}) + 38.6$ ; (Kim et al., 2010)]. The CL- $\text{TEX}_{86}$  temperatures derived from either the SPM or the surface sediments were close to the satellite-based annual mean SWT in the river water and mixing water, station R and M, respectively; whereas CL- $\text{TEX}_{86}$  temperatures for the seawater station S were lower than the winter mean SWT (**Figure 2**). The correspondence between the CL- $\text{TEX}_{86}$  temperatures derived from SPM and sediment samples ( $R^2 = 0.70$ ,  $P < 0.01$ ) along the salinity gradient indicated that the  $\text{TEX}_{86}$  signal in the sediment predominantly reflected archaea from the water column, which is consistent with previous studies



in the PR estuary (Wang et al., 2015) and other coastal settings (Herfort et al., 2006; Zell et al., 2014).

Total IPL- $\text{TEX}_{86}$  temperatures in the water column were consistently lower than both the June mean SWT and *in situ* measurements, although the sampling season was summer (Figure 2). In the mixing water and seawater, the phospho IPL- $\text{TEX}_{86}$  was lower than the total IPL- $\text{TEX}_{86}$  whereas it was very close to the CL- $\text{TEX}_{86}$  (Figure 2; Table 1). Since phosphatidyl head groups can be degraded faster than the glycosidic head groups, the phospho IPL is considered to be a better reflection of the living microorganisms (Harvey et al., 1986; Schouten et al., 2010), which may explain the deviation between these IPL pools. Relatively rapid conversion of phospho IPL to CL may result in more similar ring distributions and thus  $\text{TEX}_{86}$  values between phospho IPL and CL. Furthermore, in the same study area, the variability in  $\text{TEX}_{86}$  was suggested to be due to changes in archaeal community composition in the water column, in which the unusually low  $\text{TEX}_{86}$ -derived temperature in the coastal SCS was speculated to be linked to MG-II *Euryarchaeota* (Wang et al., 2015).

Since  $\text{TEX}_{86}$  can be influenced by factors other than temperature, the ring index was proposed to evaluate the accuracy of  $\text{TEX}_{86}$  in marine sediments (Zhang et al., 2016). Here, CL-, phospho IPL-, and total IPL- $\text{TEX}_{86}$  values were plotted against  $\text{RI}_1$  (Equation 2; Figure 3) using data derived from the SPM and surface sediment samples collected during the current and previous studies (Wei et al., 2011; Ge et al., 2013; Zhang et al., 2013; Wang et al., 2015). Most SPM and surface sediment samples from the open South China Sea plotted within

the  $\text{RI}_1$ - $\text{TEX}_{86}$ -confined zone [ $\text{RI}_1 = 3.32 \times (\text{TEX}_{86})^2 - 0.77 \times \text{TEX}_{86} + 1.59, \pm 2\sigma \sim 0.3$ ; (Zhang et al., 2016)], whereas the majority of samples from coastal SCS and the PR estuary fell above the calibration zone (Figure 3), exhibiting higher ring index values than those from the open SCS. This implies that the GDGT pool in the water column of the PR estuary and coastal SCS comprised relatively more cyclopentane rings than predicted from the measured SWT. If it is assumed that GDGTs produced only by *Thaumarchaeota* underpin the relationship between SWT and  $\text{TEX}_{86}$  (e.g., Schouten et al., 2002), then it follows that either *Thaumarchaeota* in the PR estuary respond differently to temperature than marine strains, or there is another source of cycloalkyl-containing GDGTs in the estuary.

To further assess the distribution of RI values in the SPM and to explore other contributor(s) to the cyclopentyl GDGT pool in the study area, mean values of CL-, total IPL-, and phospho IPL-ring index were examined (Figure 4). Note that crenarchaeol, a biomarker for MG-I *Thaumarchaeota*, was excluded from the ring index calculation ( $\text{RI}_2$ , Equation 3) in order to limit its overwhelming influence on the index. The re-defined  $\text{RI}_2$  equation is more sensitive to the variation of cyclopentane-containing GDGTs that might be contributed by other archaea. Compared with the river water and seawater, the highest  $\text{RI}_2$  value for either CL (avg.  $0.39 \pm 0.08$ ) or IPL (avg.  $0.48 \pm 0.07$  for total IPL; avg.  $0.47 \pm 0.10$  for phospho IPL) occurred at station M in the mixing water (Figure 4; Table 1), suggesting that the PR estuary (station M) appeared to be a hot spot of production of GDGTs with cyclopentane moieties. Further confirmation came from the comparison of %GDGT 1–4 in different water

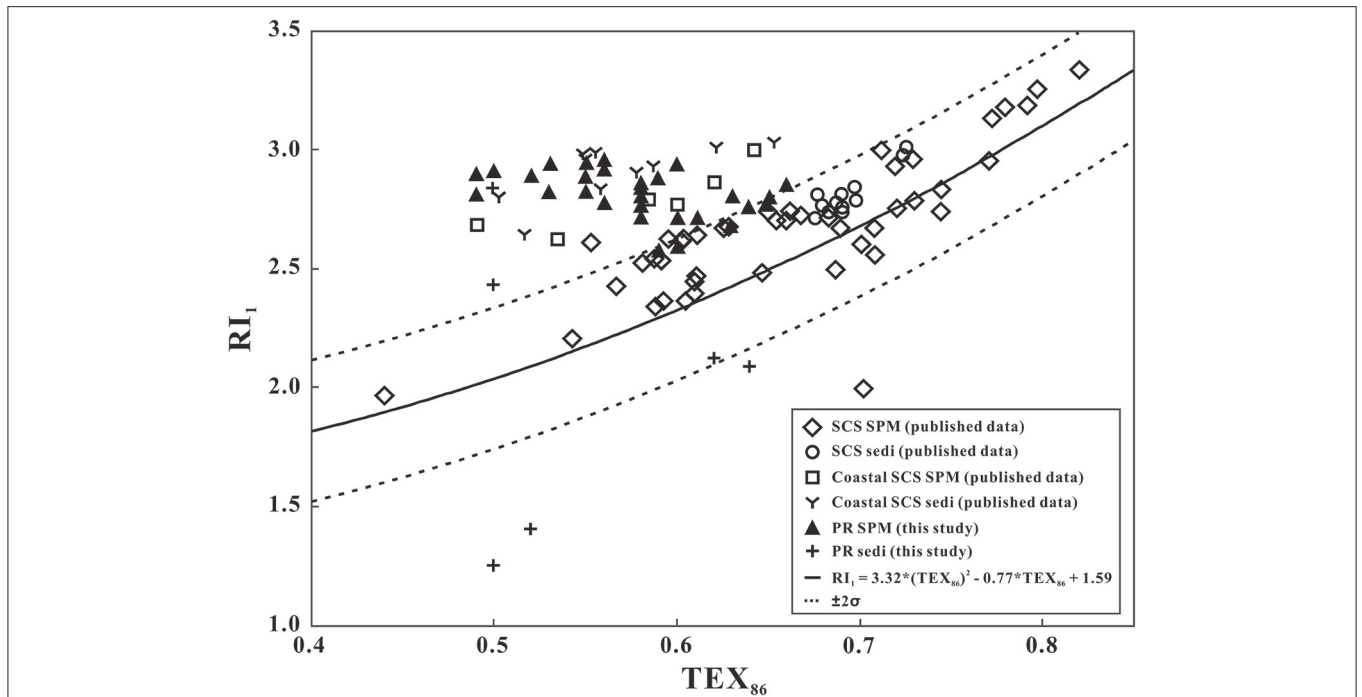


**FIGURE 3** | TEX<sub>86</sub> of the PR SPM samples and PR surface sediments plotted against RI<sub>1</sub>. The solid curve represents the RI-TEX<sub>86</sub> calibration from Zhang et al. (2016). The SCS SPM/sediments and coastal SCS SPM/sediments are from Wei et al. (2011), Ge et al. (2013), Zhang et al. (2013), and Wang et al. (2015).

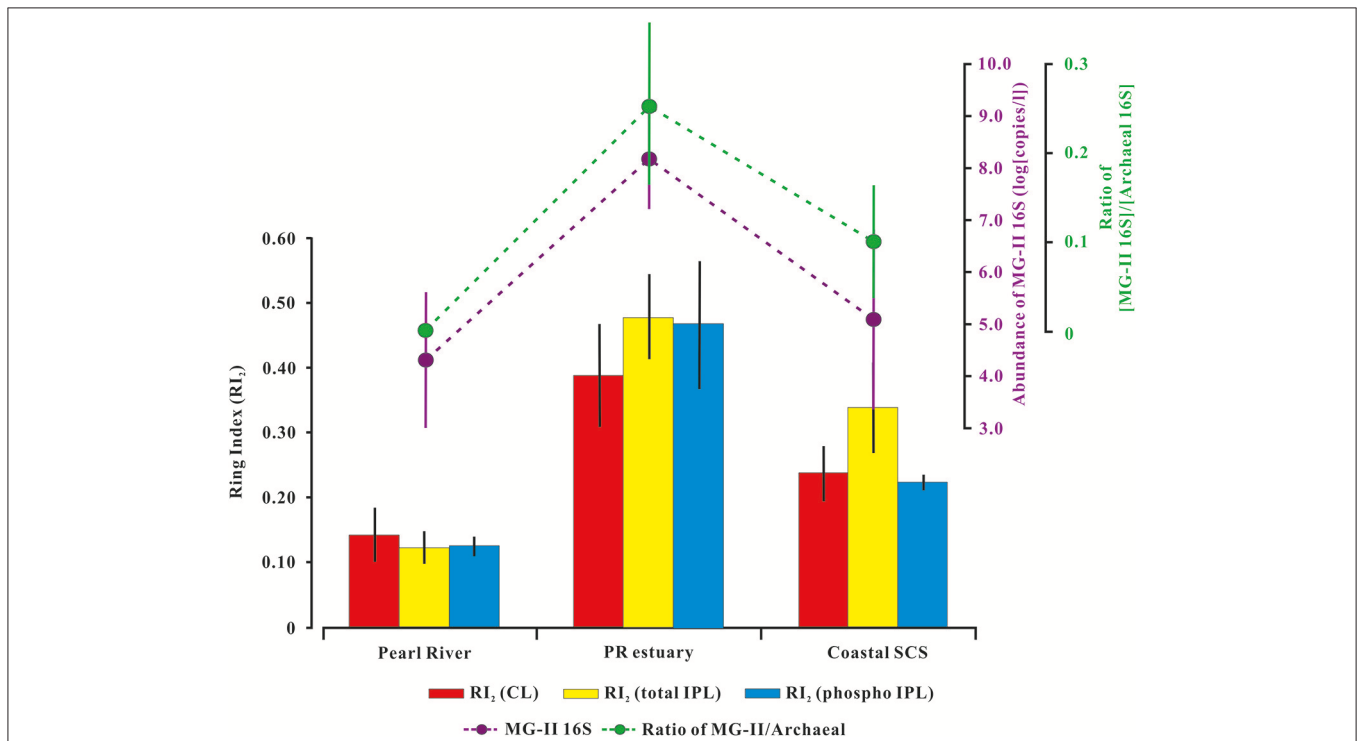


**FIGURE 4** | Distribution of the mean values of Ring Index (RI<sub>2</sub>) compared with the abundance of MG-II *Euryarchaeota* 16S rRNA gene and the gene abundance ratio of MG-II *Euryarchaeota* to total archaea along the salinity gradient from the river water to seawater. RI (Equation 3) was calculated from CL (red bars), total-IPL (yellow bars), and phospho-IPL (blue bars). Details are shown in **Table 1**.

settings (Table S1), which showed that the sum of the fractional abundances of the GDGTs with 1–4 cyclopentane moieties in the mixing water was significantly higher than that in the seawater or river water. In the mixing water station, the mean values of total IPL-RI and phospho IPL-RI were not significantly different; both were higher than the CL-RI (Figure 4). In the seawater station, however, the total IPL-RI ( $0.34 \pm 0.07$ ) was more elevated than the phospho IPL-RI ( $0.22 \pm 0.01$ ) and the CL-RI ( $0.24 \pm 0.04$ ; Figure 4). This ring index distribution pattern at station S corresponded to the  $\text{TEX}_{86}$ -temperature distribution in the SPM and sediment samples (Figure 2), suggesting that cyclopentane-containing GDGTs altered the  $\text{TEX}_{86}$  record in the water column, and the vertical transportation of GDGTs from the water column appeared to be a predominant source to the sediment.

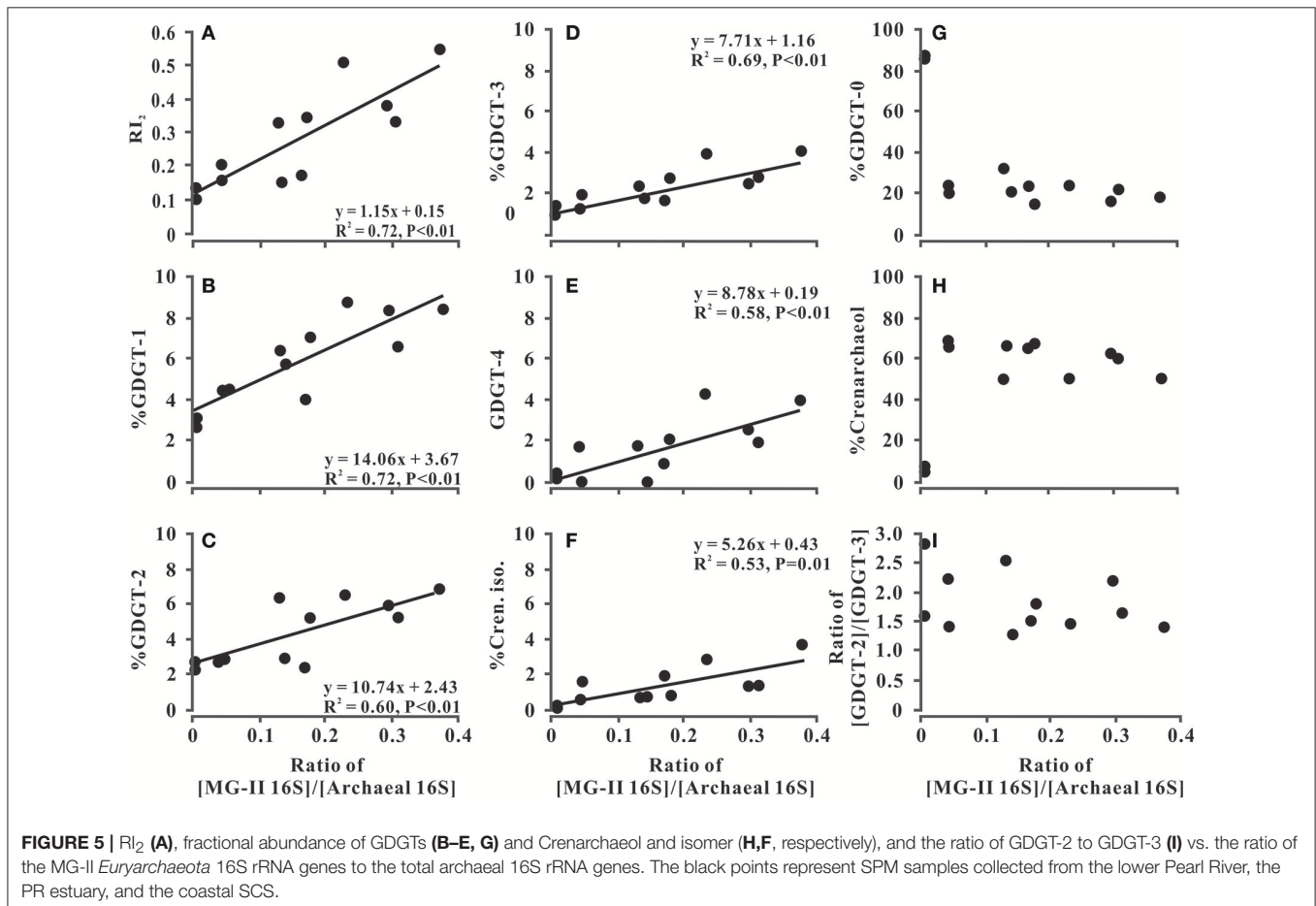
## Relationship between MG-II *Euryarchaeota* and Cyclopentane-Containing GDGTs

Previous studies reported that a significant proportion of MG-II *Euryarchaeota* was diversely present in the estuarine and coastal regions, including the Pearl River estuary (Liu et al., 2014; Wang et al., 2015), the Yangtze River estuary (Liu M. et al., 2011), and the Jiulong River estuary (Hu et al., 2015). In this study, the MG-II *Euryarchaeota* 16S rRNA gene averaged  $5.4 \pm 5.9 \times 10^8$  copies  $\text{L}^{-1}$  ( $n = 6$ ) at the mixing water station, which was two to three

orders of magnitude higher than that in river water station (avg.  $1.5 \pm 2.1 \times 10^5$  copies  $\text{L}^{-1}$ ,  $n = 2$ ) and seawater station (avg.  $4.9 \pm 9.4 \times 10^6$  copies  $\text{L}^{-1}$ ,  $n = 4$ ; Figure 4). Considering the heterotrophic life style of MG-II, which have been demonstrated by the former genetic analysis (Iverson et al., 2012; Li et al., 2015; Martin-Cuadrado et al., 2015) and cultivation experiment (Orsi et al., 2015, 2016), the high abundances of MG-II in the mixing water station seem to be due to the high phototrophs that enhanced by nutrients input from upper river (Gan et al., 2014).

The ratio of MG-II *Euryarchaeota* 16S rRNA gene abundance to total archaeal 16S rRNA gene abundance ( $[\text{MG-II } 16\text{S}]/[\text{Archaea } 16\text{S}]$ ) in mixing water (avg.  $0.25 \pm 0.08$ ,  $n = 6$ ) was significantly higher than in the seawater (avg.  $0.10 \pm 0.004$ ,  $n = 4$ ;  $P < 0.01$ ), whereas it was negligible (avg.  $<0.0001$ ) in the river water (Figure 4). This observation was also supported by pyrosequencing analysis, which exhibited a linear correlation with the qPCR-based ratio of  $[\text{MG-II}]/[\text{Archaea } 16\text{S}]$  (Figure S2; Table S2). These results further confirmed that the PR estuary (mixing zone, salinity avg. 16.6) provided a habitat to sustain a natural enrichment of planktonic MG-II *Euryarchaeota*.

The presence of (more labile) phospho IPL-GDGTs implied *in situ* production of isoprenoidal GDGTs in the water column along the entire salinity gradient from the Pearl River to coastal SCS. The elevated phospho IPL-RI in the mixing water



additionally suggests that higher relative proportions of GDGTs with 1–4 cyclopentane moieties were produced in the PR estuary. A linear regression analysis confirmed the positive relationship between phospho IPL-derived RI and the [MG-II 16S]/[Archaea 16S] ratio in the water column along the salinity gradient ( $R^2 = 0.72$ ,  $P < 0.01$ ; **Figure 5A**). Therefore, it is reasonable to hypothesize that MG-II *Euryarchaeota* preferentially synthesized GDGTs with 1–4 cyclopentane moieties in this region. Moreover, production of GDGTs-1 to -4 by MG-II *Euryarchaeota* could represent the missing source needed to explain the elevated value of RI and deviation from the RI-TEX<sub>86</sub> relationship driven by the preservation of *Thaumarchaeota* GDGTs in global core-top sediments.

To further constrain the relationship between MG-II *Euryarchaeota* and cyclopentane-containing GDGTs, linear regression analysis was conducted between the fractional abundance of GDGTs and the [MG-II 16S]/[Archaea 16S] ratio in the SPM along the salinity gradient. Results exhibited a significantly positive linear correlation between the [MG-II 16S]/[Archaea 16S] ratio and the fractional abundance of phospho IPL-based GDGT with cyclopentane moieties (**Figures 5B–F**). In contrast, we observed no correlation between the [MG-II 16S]/[Archaea 16S] ratio and the fractional abundances of phospho IPL-based GDGT-0 or crenarchaeol (**Figures 5G,H; Table 2**). Similar trends of the linear correlations were also observed between the [MG-II 16S]/[Archaea 16S] ratio and the CL- and total IPL-GDGTs with 1–4 cyclopentane moieties, with a less significant correlation between the [MG-II 16S]/[Archaea 16S] ratio and the total IPL-based crenarchaeol regioisomer (**Table 2**). Although MG-II *Euryarchaeota* were suggested to be an alternative source of crenarchaeol in the ocean (Lincoln et al., 2014a), our study showed an absence of a significant correlation between the distribution of MG-II *Euryarchaeota* and crenarchaeol (**Figure 5H**). However, members of MG-II *Euryarchaeota* living in the North Pacific Subtropical Gyre (i.e., those targeted by Lincoln et al., 2014a) may be different from those living in the coastal zone of the PR estuary. This is consistent with the phylogenetic distribution of MG-II reported by Wang et al. (2015), which showed diverse groups of MG-II living in this region.

By comparison of the  $R^2$  values and slopes of the regression equations (**Figures 5B–F**), GDGT-1 exhibited not only the strongest correlation with MG-II *Euryarchaeota* in the study area, but also largest relative enrichment (i.e., slope of 14.06). If MG-II *Euryarchaeota* preferentially synthesized GDGT-1, additional contribution of GDGT-1 to the water column of the PR estuary and the coastal SCS would be reflected by an increase in RI values and a substantial decrease in TEX<sub>86</sub> values. Offsets in TEX<sub>86</sub> values have been similarly proposed to result from the decreased ratio of GDGT-2 to GDGT-3 in the surface sediments of this area (Wang et al., 2015), whereas the increased ratio of GDGT-2 over GDGT-3 in the deep-water column seems to be responsible for a warm bias of TEX<sub>86</sub>-derived temperature in other marine environments (Taylor et al., 2013; Hernandez-Sanchez et al., 2014). In this study, however, no correlation is exhibited between GDGT-2/3 ratio and [MG-II 16S]/[Archaea 16S] ratio (**Figure 5I**). A recent study by Kim et al.

**TABLE 2** | Regression analysis between the ratio of MG-II 16S rRNA genes to Archaeal 16S rRNA genes vs. the fractional abundance of GDGTs, ring index (RI<sub>2</sub>), and the ratio of GDGT-2 to GDGT-3.

	[MG-II/Archaea] vs. CL <sup>a</sup>		[MG-II/Archaea] vs. total-IPL		[MG-II/Archaea] vs. phospho-IPL	
	R <sup>2</sup>	P-value	R <sup>2</sup>	P-value	R <sup>2</sup>	P-value
%GDGT-0	0.37	0.04	0.44	0.02	0.40	0.03
%GDGT-1	0.50	0.01	0.58	0.00	0.72	0.00
%GDGT-2	0.43	0.02	0.47	0.01	0.60	0.00
%GDGT-3	0.33	0.05	0.51	0.01	0.69	0.00
%GDGT-4	0.43	0.02	0.46	0.02	0.58	0.00
%Cren.	0.25	0.10	0.37	0.03	0.21	0.13
%Cren.iso	0.56	0.01	0.11	0.80	0.53	0.01
RI <sub>2</sub>	0.49	0.01	0.50	0.01	0.72	0.00
GDGT 2/3	0.13	0.25	0.30	0.07	0.11	0.29

<sup>a</sup>[MG-II/Archaea], the 16S rRNA gene ratio of MG-II to archaeal. CL, core lipids; total-IPL, intact polar lipids derived upon acid hydrolysis; phospho-IPL, intact polar lipids derived upon base hydrolysis.

(2015) suggested that coincident increases in GDGT-2 and the crenarchaeol regioisomer and decreases in GDGT-1 and GDGT-3 shifted TEX<sub>86</sub>-derived temperatures toward higher values in the deep-water surface sediments of the Mediterranean Sea. In combination with our data (**Figures 4, 5**), these observations are consistent with the interpretation that planktonic *Euryarchaeota* have the potential to bias TEX<sub>86</sub> by changing the distribution of TEX<sub>86</sub>-related GDGTs (especially those with 1–3 cyclopentane rings) in different marine environments.

## CONCLUSIONS

This study assessed the relationship between TEX<sub>86</sub>-related GDGTs and MG-II *Euryarchaeota* along a salinity gradient from river water to seawater. The fractional abundance of MG-II *Euryarchaeota* was correlated with %GDGTs with cyclopentane moieties as well as ring index values, implying that MG-II *Euryarchaeota* may contribute ringed GDGTs to the total GDGT pool. This source would thus increase the ring index value and potentially bias the TEX<sub>86</sub> proxy. However, MG-II *Euryarchaeota* living in the estuary and coastal region did not seem to be a significant source of crenarchaeol. These and other findings based on environmental distributions provide indirect evidence of the lipid profile of MG-II *Euryarchaeota*, which cannot be validated until a pure culture is available.

## AUTHOR CONTRIBUTIONS

JW and CZ designed this study. JW extracted and analyzed lipids. WX extracted and analyzed DNA. JW, WX, YZ, TM, and CZ wrote the paper.

## ACKNOWLEDGMENTS

We thank Huangmin Ge, Geng Wu, and Chao Li for helping with the sampling. Songze Chen helped performing the qPCR analysis. We appreciate Dr. Ding He (Zhejiang Uni.) for commenting

on an earlier version of the manuscript. An early version of this manuscript was discussed online at the Biogeosciences Discussion forum (doi: 10.5194/bgd-12-12455-2015); however, the final paper was declined for publication by Biogeosciences. This research was supported by the National Key Basic Research Program of China grant #2013CB955703 and 2016YFA0601101 (CZ), and the National Science Foundation of China Grant #41530105 and 41673073 (CZ). This study is also a contribution to the international IMBER project. Comments from the two reviewers and the editor significantly improved the quality of the paper and are greatly appreciated.

## REFERENCES

- Bano, N., Ruffin, S., Ransom, B., and Hollibaugh, J. T. (2004). Phylogenetic composition of Arctic Ocean archaeal assemblages and comparison with Antarctic assemblages. *Appl. Environ. Microbiol.* 70, 781–789. doi: 10.1128/AEM.70.2.781-789.2004
- Blaga, C. I., Reichart, G. J., Heiri, O., and Sinninghe Damsté, J. S. (2009). Tetraether membrane lipid distributions in lake particulate matter and sediments: a study of 47 European lakes along a North–South transect. *J. Paleolimnol.* 41, 523–540. doi: 10.1007/s10933-008-9242-2
- Bligh, E. G., and Dyer, W. J. (1959). A rapid method of total lipid extraction and purification. *Can. J. Biochem. Physiol.* 37, 911–917. doi: 10.1139/y59-099
- Caporaso, J. G., Kuczynski, J., Stombaugh, J., Bittinger, K., Bushman, F. D., Costello, E. K., et al. (2010). QIIME allows analysis of high-throughput community sequencing data. *Nat. Methods* 7, 335–336. doi: 10.1038/nmeth.f.303
- Cole, J. R., Wang, Q., Cardenas, E., Fish, J., Chai, B., Farris, R. J., et al. (2009). The Ribosomal Database Project: improved alignments and new tools for rDNA analysis. *Nucleic Acids Res.* 37, D141–D145. doi: 10.1093/nar/gkn879
- DeLong, E. F. (1992). Archaea in coastal marine environments. *Proc. Natl. Acad. Sci. U.S.A.* 89, 5685–5689. doi: 10.1073/pnas.89.12.5685
- Galand, P. E., Gutierrez-Provecho, C., Massana, R., Gasol, J., and Casamayor, E. O. (2010). Interannual recurrence of archaeal assemblages in the coastal NW Mediterranean Sea. *Limnol. Oceanogr.* 55, 2117–2125. doi: 10.4319/lo.2010.55.5.2117
- Gan, J., Lu, Z., Cheung, A., Dai, M., Liang, L., Harrison, P. J., et al. (2014). Assessing ecosystem response to phosphorus and nitrogen limitation in the Pearl River plume using the Regional Ocean Modeling System (ROMS). *J. Geophys. Res.* 119, 8858–8877. doi: 10.1002/2014JC009951
- Gantner, S., Andersson, A. F., Alonso-Saez, L., and Bertilsson, S. (2011). Novel primers for 16S rDNA-based archaeal community analyses in environmental samples. *J. Microbiol. Methods* 84, 12–18. doi: 10.1016/j.mimet.2010.10.001
- Ge, H., Zhang, C. L., Dang, H. Y., Zhu, C., and Jia, G. D. (2013). Distribution of tetraether lipids in surface sediments of the northern South China Sea: implications for TEX<sub>86</sub> proxies. *Geosci. Front.* 4, 223–229. doi: 10.1016/j.gsf.2012.10.002
- Harvey, H. R., Fallon, R. D., and Patton, J. S. (1986). The effect of organic matter and oxygen on the degradation of bacterial membrane lipids in marine sediments. *Geochim. Cosmochim. Acta* 50, 795–804. doi: 10.1016/0016-7037(86)90355-8
- Herfort, L., Schouten, S., Boon, J. P., and Sinninghe Damsté, J. S. (2006). Application of the TEX<sub>86</sub> temperature proxy in the southern North Sea. *Org. Geochem.* 37, 1715–1726. doi: 10.1016/j.orggeochem.2006.07.021
- Hernandez-Sanchez, M. T., Woodward, E. M. S., Taylor, K. W. R., Henderson, G. M., and Pancost, R. D. (2014). Variations in GDGT distributions through the water column in the South East Atlantic Ocean. *Geochim. Cosmochim. Acta* 132, 337–348. doi: 10.1016/j.gca.2014.02.009
- Hugoni, M., Taib, N., Debroas, D., Domaizon, I., Dufournel, I. J., Bronner, G., et al. (2013). Structure of the rare archaeal biosphere and seasonal dynamics of active ecotypes in surface coastal waters. *Proc. Natl. Acad. Sci. U.S.A.* 110, 6004–6009. doi: 10.1073/pnas.1216863110
- Hu, A., Hou, L., and Yu, C.-P. (2015). Biogeography of planktonic and benthic archaeal communities in a subtropical eutrophic estuary of China. *Microbiol. Ecol.* 70, 322–355. doi: 10.1007/s00248-015-0597-4
- Huguet, C., Hopmans, E. C., Febo-Ayala, W., Thompson, D. H., Sinninghe Damsté, J. S., and Schouten, S. (2006). An improved method to determine the absolute abundance of glycerol dibiphytanyl glycerol tetraether lipids. *Org. Geochem.* 37, 1036–1041. doi: 10.1016/j.orggeochem.2006.05.008
- Iverson, V., Morris, R. M., Frazar, C. D., Berthiaume, C. T., Morales, R. L., and Armbrust, E. V. (2012). Untangling genomes from metagenomes: revealing an uncultured class of marine Euryarchaeota. *Science* 335, 587–590. doi: 10.1126/science.1212665
- Karner, M., DeLong, E. F., and Karl, D. M. (2001). Archaeal dominance in the mesopelagic zone of the Pacific Ocean. *Nature* 409, 507–510. doi: 10.1038/35054051
- Kim, J.-H., Schouten, S., Hopmans, E. C., Donner, B., and Sinninghe Damsté, J. S. (2008). Global core-top calibration of the TEX<sub>86</sub> paleothermometer in the ocean. *Geochim. Cosmochim. Acta* 72, 1154–1173. doi: 10.1016/j.gca.2007.12.010
- Kim, J.-H., van der Meer, J., Schouten, S., Helmke, P., Willmott, V., Sangiorgi, F., et al. (2010). New indices and calibrations derived from the distribution of crenarchaeal isoprenoid tetraether lipids: implications for past sea surface temperature reconstructions. *Geochim. Cosmochim. Acta* 74, 4639–4654. doi: 10.1016/j.gca.2010.05.027
- Kim, J. H., Schouten, S., Rodrigo-Gamiz, M., Rampen, S., Marino, G., Huguet, C., et al. (2015). Influence of deep-water derived isoprenoid tetraether lipids on the TEX<sub>86</sub> paleothermometer in the Mediterranean Sea. *Geochim. Cosmochim. Acta* 150, 125–141. doi: 10.1016/j.gca.2014.11.017
- Lee, K. E., Kim, J.-H., Wilke, I., Helmke, P., and Schouten, S. (2008). A study of the alkenone, TEX<sub>86</sub>, and planktonic foraminifera in the Benguela Upwelling System: Implications for past sea surface temperature estimates. *Geochem. Geophys. Geosyst.* 9:Q10019. doi: 10.1029/2008GC002056
- Li, M., Baker, B. J., Anantharaman, K., Jain, S., Breier, J. A., and Dick, G. J. (2015). Genomic and transcriptomic evidence for scavenging of diverse organic compounds by widespread deep-sea archaea. *Nat. Commun.* 6:8933. doi: 10.1038/ncomms9933
- Liu, M., Xiao, T., Wu, Y., Zhou, F., and Zhang, W. (2011). Temporal distribution of the archaeal community in the Changjiang Estuary hypoxia area and the adjacent East China Sea as determined by denaturing gradient gel electrophoresis and multivariate analysis. *Can. J. Microbiol.* 57, 504–513. doi: 10.1139/w11-037
- Liu, J., Yu, S., Zhao, M., He, B., and Zhang, X.-H. (2014). Shifts in archaea plankton community structure along ecological gradients of Pearl Estuary. *FEMS Microbiol. Ecol.* 90, 424–435. doi: 10.1111/1574-6941.12404
- Liu, X. L., Lipp, J. S., and Hinrichs, K.-U. (2011). Distribution of intact and core GDGTs in marine sediments. *Org. Geochem.* 42, 368–375. doi: 10.1016/j.orggeochem.2011.02.003
- Lincoln, S. A., Wai, B., Eppley, J. M., Church, M. J., Summons, R. E., and DeLong, E. F. (2014a). Planktonic Euryarchaeota are a significant source of archaeal tetraether lipids in the ocean. *Proc. Natl. Acad. Sci. U.S.A.* 111, 9858–9863. doi: 10.1073/pnas.1409439111
- Lincoln, S. A., Wai, B., Eppley, J. M., Church, M. J., Summons, R. E., and DeLong, E. F. (2014b). Reply to Schouten et al.: marine Group II planktonic Euryarchaeota are significant contributors to tetraether lipids in the ocean. *Proc. Natl. Acad. Sci. U.S.A.* 111:E4286. doi: 10.1073/pnas.1416736111
- Martin-Cuadrado, A.-B., Garcia-Heredia, I., Moltó A. G., López-Ubeda, R., Kimes, N., López-García, P., et al. (2015). A new class of marine Euryarchaeota group

## SUPPLEMENTARY MATERIAL

The Supplementary Material for this article can be found online at: <https://www.frontiersin.org/articles/10.3389/fmicb.2017.02077/full#supplementary-material>

**Figure S1** | Structures of archaeal core GDGTs described in the text.

**Figure S2** | Relationship of fractional abundances of MG-II *Euryarchaeota* derived from quantitative polymerase chain reaction (qPCR) and pyrosequencing. % MG-II (qPCR) is calculated based on the ratio of MG-II 16S rRNA gene to Archaea 16S rRNA gene; % MG-II (sequencing) refers to the fractional abundance of the MG-II OTUs to the total archaeal OTUs.

- II from the mediterranean deep chlorophyll maximum. *ISME J.* 9, 1619–1634. doi: 10.1038/ismej.2014.249
- Massana, R., Murray, A. E., Preston, C. M., and DeLong, E. F. (1997). Vertical distribution and phylogenetic characterization of marine planktonic Archaea in the Santa Barbara Channel. *Appl. Environ. Microbiol.* 63, 50–56.
- Orsi, W. D., Smith, J. M., Wilcox, H. M., Swallow, J. E., Carini, P., Worden, A. Z., et al. (2015). Ecophysiology of uncultivated marine euryarchaea is linked to particulate organic matter. *ISME J.* 9, 1747–1763. doi: 10.1038/ismej.2014.260
- Orsi, W. D., Smith, J. M., Liu, S., Liu, Z., Sakamoto, C. M., Wilken, S., et al. (2016). Diverse, uncultivated bacteria and archaea underlying the cycling of dissolved protein in the ocean. *ISME J.* 10, 2158–2173. doi: 10.1038/ismej.2016.20
- Pitcher, A., Hopmans, E. C., Schouten, S., and Sinninghe Damsté, J. S. (2009). Separation of core and intact polar archaeal tetraether lipids using silica columns: insights into living and fossil biomass contributions. *Org. Geochem.* 40, 12–19. doi: 10.1016/j.orggeochem.2008.09.008
- Pitcher, A., Hopmans, E. C., Mosier, A. C., Francis, C. A., Reese, S. K., Schouten, S., et al. (2011a). Distribution of core and intact polar tetraether lipids in enrichment cultures of Thaumarchaeota from marine sediments. *Appl. Environ. Microbiol.* 77, 3468–3477.
- Pitcher, A., Villanueva, L., Hopmans, E. C., Schouten, S., Reichart, G. J., and Sinninghe Damsté, J. S. (2011b). Niche segregation of ammonia-oxidizing archaea and anammox bacteria in the Arabian Sea oxygen minimum zone. *ISME J.* 5, 1896–1904. doi: 10.1038/ismej.2011.60
- Schloss, P. D., Westcott, S. L., Ryabin, T., Hall, J. R., Hartmann, M., Hollister, E. B., et al. (2009). Introducing mothur: opensource, platform-independent, community-supported software for describing and comparing microbial communities. *Appl. Environ. Microbiol.* 75, 7537–7541. doi: 10.1128/AEM.01541-09
- Schouten, S., Hopmans, E. C., Schefuß, E., and Sinninghe Damsté, J. S. (2002). Distributional variations in marine crenarchaeotal membrane lipids: a new tool for reconstructing ancient sea water temperatures? *Earth Planet. Sci. Lett.* 204, 265–274. doi: 10.1016/S0012-821X(02)00979-2
- Schouten, S., Huguet, C., Hopmans, E. C., and Sinninghe Damsté, J. S. (2007). Improved analytical methodology of the TEX<sub>86</sub> paleothermometry by high performance liquid chromatography/atmospheric pressure chemical ionization–mass spectrometry. *Anal. Chem.* 79, 2940–2944. doi: 10.1021/ac062339v
- Schouten, S., Hopmans, E. C., Baas, M., Boumann, H., Standfest, S., Könneke, M., et al. (2008). Intact membrane lipids of “Candidatus Nitrosopumilus maritimus”, a cultivated representative of the cosmopolitan mesophilic Group I Crenarchaeota. *Appl. Environ. Microbiol.* 74, 2433–2440. doi: 10.1128/AEM.01709-07
- Schouten, S., Middelburg, J. J., Hopmans, E. C., and Sinninghe Damsté, J. S. (2010). Fossilization and degradation of intact polar lipids in deep subsurface sediments: a theoretical approach. *Geochim. Cosmochim. Acta* 74, 3806–3814. doi: 10.1016/j.gca.2010.03.029
- Schouten, S., Hopmans, E. C., and Sinninghe Damsté, J. S. (2013). The organic geochemistry of glycerol dialkyl glycerol tetraether lipids: a review. *Org. Geochem.* 54, 19–61. doi: 10.1016/j.orggeochem.2012.09.006
- Schouten, S., Villanueva, L., Hopmans, E. C., van der Meer, M. T. J., and Sinninghe Damsté, J. S. (2014). Are Marine Group II Euryarchaeota significant contributors to tetraether lipids in the ocean? *Proc. Natl. Acad. Sci. U.S.A.* 111:E4285. doi: 10.1073/pnas.1416176111
- Sinninghe Damsté, J. S., Hopmans, E. C., Schouten, S., van Duin, A. C. T., and Genevassen, J. A. J. (2002). Crenarchaeol: the characteristic core glycerol dibiphytanyl glycerol tetraether membrane lipid of cosmopolitan pelagic crenarchaeota. *J. Lipid Res.* 43, 1641–1651. doi: 10.1194/jlr.M200148-JLR200
- Sinninghe Damsté, J. S., Ossebaar, J., Schouten, S., and Verschuren, D. (2012). Distribution of tetraether lipids in the 25-kyr sedimentary record of Lake Challa: extracting reliable TEX<sub>86</sub> and MBT/CBT palaeotemperatures from an equatorial African lake. *Quat. Sci. Rev.* 50, 43–54. doi: 10.1016/j.quascirev.2012.07.001
- Strong, D. J., Flecker, R., Valdes, P. J., Wilkinson, I. P., Rees, J. G., Zong, Y. Q., et al. (2012). Organic matter distribution in the modern sediments of the Pearl River Estuary. *Org. Geochem.* 49, 68–82. doi: 10.1016/j.orggeochem.2012.04.011
- Taylor, K. W. R., Huber, M., Hollis, C. J., Hernandez-Sanchez, M. T., and Pancost, R. D. (2013). Reevaluating modern and palaeogene GDGT distributions: implications for SST reconstructions. *Global Planet. Change* 108, 158–174. doi: 10.1016/j.gloplacha.2013.06.011
- Teira, E., Reinthaler, T., Pernthaler, A., Pernthaler, J., and Herndl, G. J. (2004). Combining catalyzed reporter deposition–fluorescence *in situ* hybridization and microautoradiography to detect substrate utilization by Bacteria and Archaea in the deep ocean. *Appl. Environ. Microbiol.* 70, 4411–4414. doi: 10.1128/AEM.70.7.4411-4414.2004
- Turich, C., Freeman, K. H., Bruns, M. A., Conte, M., Jones, A. D., and Wakeham, S. G. (2007). Lipids of marine Archaea: patterns and provenance in the water-column and sediments. *Geochim. Cosmochim. Acta* 71, 3272–3291. doi: 10.1016/j.gca.2007.04.013
- Wang, J.-X., Wei, Y., Wang, P., Hong, Y., and Zhang, C. L. (2015). Unusually low TEX<sub>86</sub> values in the transitional zone between Pearl River estuary and coastal South China Sea: impact of changing archaeal community composition. *Chem. Geol.* 402, 18–29. doi: 10.1016/j.chemgeo.2015.03.002
- Wei, Y., Wang, J. X., Liu, J., Dong, L., Li, L., Wang, H., et al. (2011). Spatial variations in Archaeal lipids of surface water and core-top sediments in the South China Sea: implications for paleoclimate studies. *Appl. Environ. Microbiol.* 77, 7479–7489. doi: 10.1128/AEM.00580-11
- Weijers, J. W. H., Schouten, S., Spaargaren, O. C., and Sinninghe Damsté, J. S. (2006). Occurrence and distribution of tetraether membrane in soils: implications for the use of the BIT index and the TEX<sub>86</sub> SST proxy. *Org. Geochem.* 37, 1680–1693. doi: 10.1016/j.orggeochem.2006.07.018
- Weijers, J. W. H., Lima, K. H. L., Aquilina, A., Sinninghe Damsté, J. S., and Pancost, R. D. (2011a). Biogeochemical controls on glycerol dialkyl glycerol tetraether lipid distributions in sediments characterized by diffusive methane flux. *Geochim. Geophys. Geosyst.* 12:10. doi: 10.1029/2011GC003724
- Weijers, J. W. H., Bernhardt, B., Peterse, F., Werne, J. P., Dungait, J. A. J., Schouten, S., et al. (2011b). Absence of seasonal patterns in MBT–CBT indices in mid-latitude soils. *Geochim. Cosmochim. Acta* 75, 3179–3190. doi: 10.1016/j.gca.2011.03.015
- Zell, C., Kim, J.-H., Hollander, D., Lorenzoni, L., Baker, P., Silva, C. G., et al. (2014). Sources and distributions of branched and isoprenoid tetraether lipids on the Amazon shelf and fan: Implications for the use of GDGT-based proxies in marine sediments. *Geochim. Cosmochim. Acta* 139, 293–312. doi: 10.1016/j.gca.2014.04.038
- Zhang, C. L., Wang, J.-X., Wei, Y., Zhu, C., Huang, L., and Dong, H. (2012). Production of branched tetraether lipids in the lower Pearl River and estuary: effects of extraction methods and impact on bGDGTs proxies. *Front. Terr. Microbiol.* 2:274. doi: 10.3389/fmicb.2011.00274
- Zhang, J., Bai, Y., Xu, S., Lei, F., and Jia, G. (2013). Alkenone and tetraether lipids reflect different seasonal seawater temperatures in the coastal northern South China Sea. *Org. Geochem.* 58, 115–120. doi: 10.1016/j.orggeochem.2013.02.012
- Zhang, Y. G., Zhang, C. L., Liu, X. L., Li, L., Hinrichs, K.-U., and Noakes, J. E. (2011). Methane Index: a tetraether archaeal lipid biomarker indicator for detecting the instability of marine gas hydrates. *Earth Planet. Sci. Lett.* 307, 525–534. doi: 10.1016/j.epsl.2011.05.031
- Zhang, Y. G., Pagani, M., and Wang, Z. (2016). Ring Index: a new strategy to evaluate the integrity of TEX<sub>86</sub> paleothermometry. *Paleoceanography* 31, 220–232. doi: 10.1002/2015PA002848
- Zhu, C., Weijers, J. W. H., Wagner, T., Pan, J. M., Chen, J. F., and Pancost, R. D. (2011). Sources and distributions of tetraether lipids in surface sediments across a large riverdominated continental margin. *Org. Geochem.* 42, 376–386. doi: 10.1016/j.orggeochem.2011.02.002

**Conflict of Interest Statement:** The authors declare that the research was conducted in the absence of any commercial or financial relationships that could be construed as a potential conflict of interest.

The reviewer FS declared a shared affiliation, with no collaboration, with several of the authors to the handling Editor.

Copyright © 2017 Wang, Xie, Zhang, Meador and Zhang. This is an open-access article distributed under the terms of the Creative Commons Attribution License (CC BY). The use, distribution or reproduction in other forums is permitted, provided the original author(s) or licensor are credited and that the original publication in this journal is cited, in accordance with accepted academic practice. No use, distribution or reproduction is permitted which does not comply with these terms.